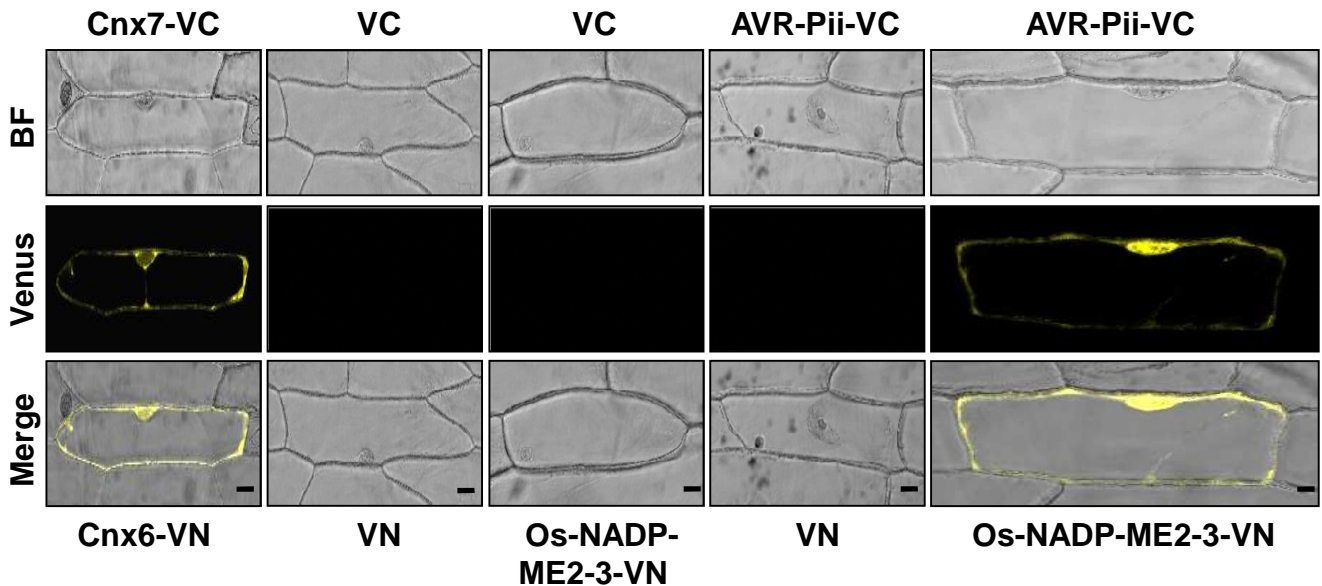


Supplementary Fig. S1. Schematic diagram of alternative splice forms of *Os-NADP-ME2*. Five different alternative splice forms of *Os-NADP-ME2* including the untranslated region (purple box), introns (black solid line), and exons (maroon box with numbers) are shown. Alternative splice forms are characterized based on the Rice Genome Annotation Project (http://rice.plantbiology.msu.edu/cgi-bin/ORF_infopage.cgi). The sequences are not drawn to scale.



Supplementary Fig. S2. Interaction between AVR-Pii and Os-NADP-ME2-3 in onion epidermal cells using BiFC. *AVR-Pii* and *Os-NADP-ME2-3* DNA constructs and the positive and negative controls were bombarded into onion epidermal cells. The signals were detected using the Venus filter (Ex/Em: 488 nm/505–550 nm wavelength) of a confocal microscope (Leica, TCS SP5). *Arabidopsis* Cnx6 and Cnx7 proteins were used as positive controls, and the empty C- and N-terminal half Venus vectors were used as negative controls. Cnx6-VN, pEXP-VYNE(R)-Cnx6; Cnx7-VC, pEXP-VYCE(R)-Cnx7; VC, pDEST-VYCE[®]_{GW}; VN, pDEST-VYNE[®]_{GW}. Scale bar, 10 μm.

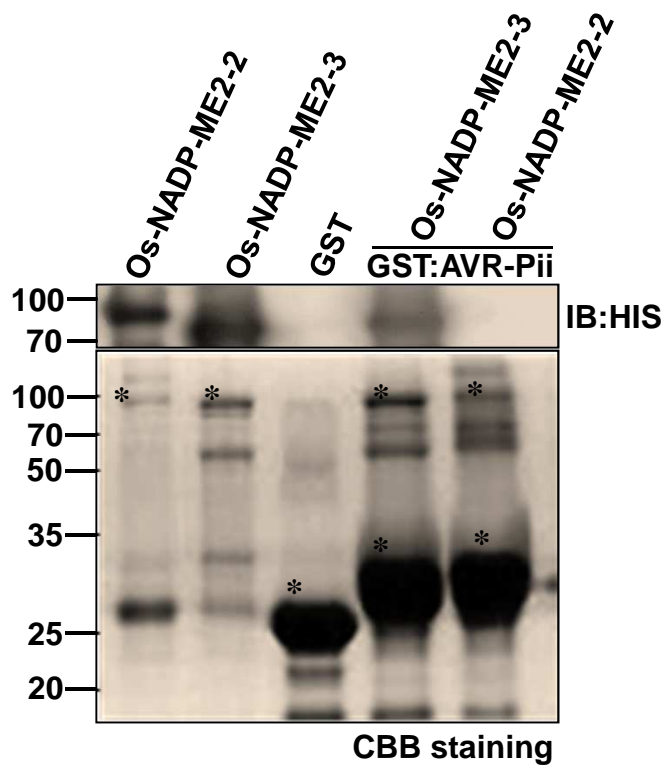
A

AVR-Pii	ATG CTT CCC ACT CCG GCC AGC CTG AAT GGC AAC ACT GAG GTC GCA
AVR-Pii-MT	ATG CTT CCC ACT CCG GCC AGC CTG AAT GGC AAC ACT GAG GTC GCA
AVR-Pii	ACC ATC TCC GAC GTT AAA CTT GAG GCC CGC AGC GAC ACC ACT TAT
AVR-Pii-MT	ACC ATC TCC GAC GTT AAA CTT GCG GCC CGC AGC GCC ACC ACT TAT
AVR-Pii	CAT AAA TGC TCC AAA TGC GGT TAT GGC AGC GAT GAT TCC GAC GCG
AVR-Pii-MT	CAT AAA TGC TCC AAA TGC GGT TAT GGC AGC GCT GCT TCC GCC GCG
AVR-Pii	TAT TTT AAT CAT AAA TGC AAC TAA
AVR-Pii-MT	TAT TTT AAT CAT AAA TGC AAC TAA

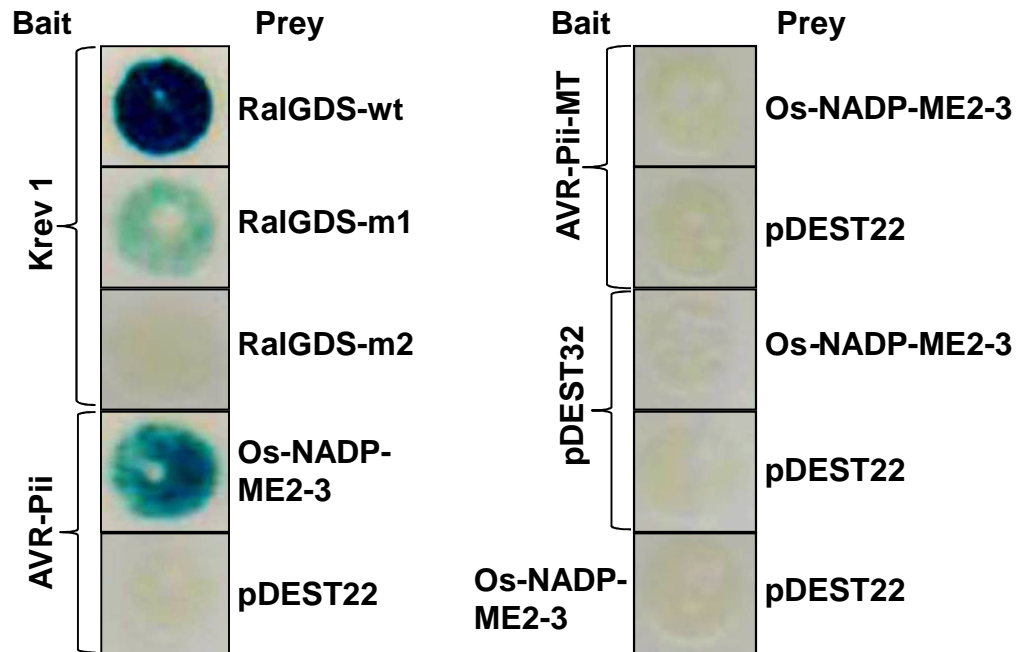
B

		E23A	D27A		D41A	D42A	D44A	
		↓	↓		↓	↓	↓	
AVR-Pii	MLPTPASLNGNTEVATISDVKLEARS	DTTYHKCSKCGYGS	DDSDAYFNH	KCN	52			
AVR-Pii-MT	MLPTPASLNGNTEVATISDVKLAARS	SATTYHKCSKCGYGS	SAASAAYFNH	KCN	52			

Supplementary Fig. S3. Site-directed mutagenesis sites within AVR-Pii sequences. Site-directed mutagenesis sites within AVR-Pii sequence. Site-directed mutagenesis was performed as described in the Materials and Methods section. (A) Nucleotide sequence alignment of AVR-Pii and mutated AVR-Pii (AVR-Pii-MT). The nucleotides in red color represented the mutated nucleotide from the AVR-Pii sequence. Five different sites were chosen for mutagenesis as shown by numbers 1, 2, 3, 4 and 5 in AVR-Pii sequence. (B) Amino acid sequence alignment of AVR-Pii and AVR-Pii-MT. The mutated sites are shown by arrows.

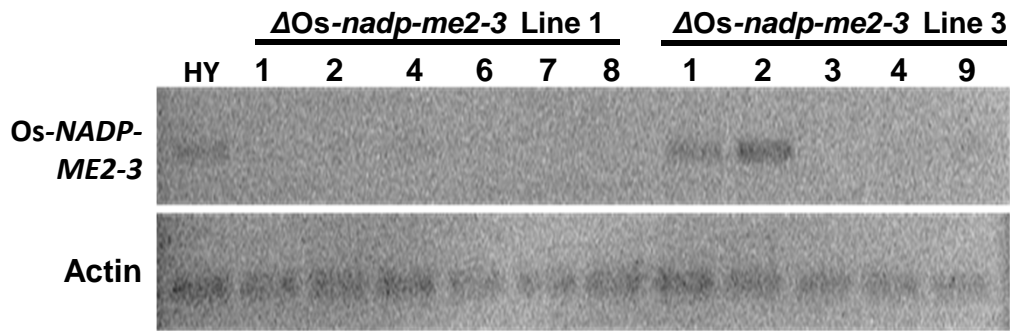


Supplementary Fig. S4. The interaction between AVR-Pii and Os-NADP-ME2-3 is specific. *In vitro* GST pull-down assay shows that GST-tagged AVR-Pii interacts only with Os-NADP-ME2-3. Both input (Os-NADP-ME2-3 and Os-NADP-ME2-2) and pull-down samples were subjected to CBB staining (lower panel) and immunoblotting (upper panel) using anti-His antibody (1:1000; ABM Inc. GO20). The asterisk (*) represents His-tagged Os-NADP-ME2-2, Os-NADP-ME2-3 (upper), and GST alone as well as GST tagged AVR-Pii (lower). IB, Immunoblotting; CBB, Coomassie Brilliant Blue.

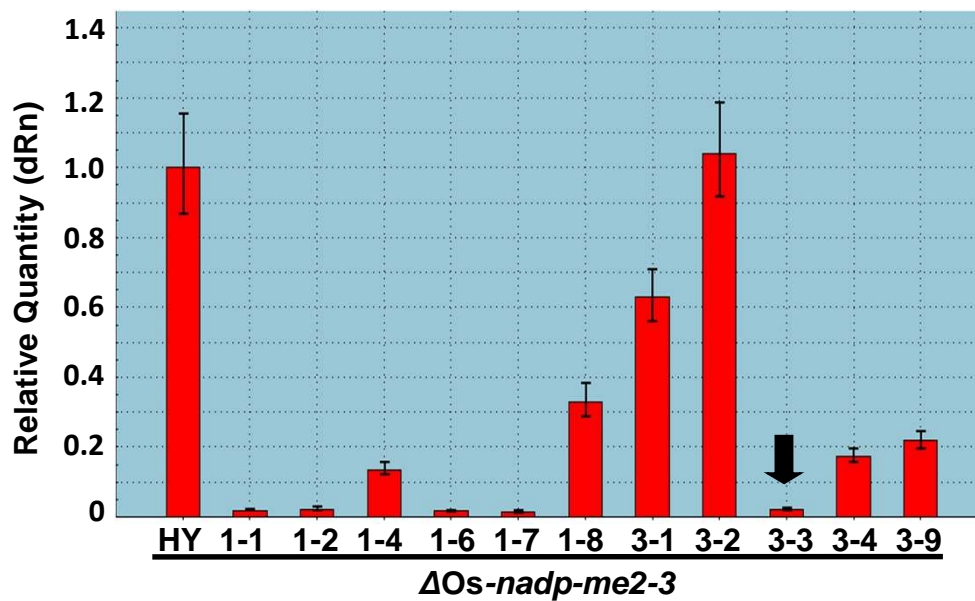


Supplementary Fig. S5. AVR-Pii mutant fails to interact with Os-NADP-ME2-3. Os-NADP-ME2-3 interacts with AVR-Pii in the yeast two-hybrid system, but it failed to interact with mutated AVR-Pii (AVR-Pii-MT). BD-AVR-Pii (bait) and BD-AVR-Pii-MT (bait) were co-transformed with AD-Os-NADP-ME2-3 (prey), and the X-gal assay was performed. Similarly, bait and prey protein were co-transformed with AD-empty and BD-empty vectors, respectively, as negative controls. Controls used were as follows: strong (pEXP32/Krev1 + pEXP22/RaIGDS-wt); weak (pEXP32/Krev1 + pEXP22/RaIGDS-m1); and absent (pEXP32/Krev1 + pEXP22/RaIGDS-m2). BD-empty vector, pDEST32; AD-empty vector, pDEST22.

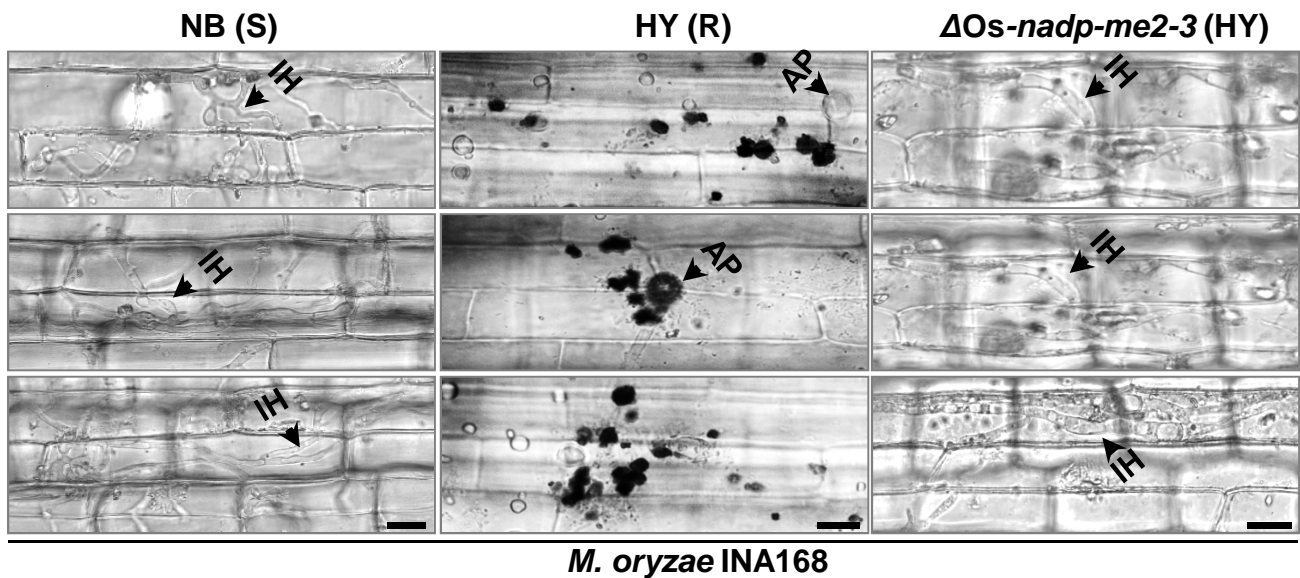
A



B



Supplementary Fig. S6. Transcript analysis of *Os-NADP-ME2-3* in HY and $\Delta Os-nadp-me2-3$ mutants using RT-PCR and quantitative RT-PCR (qPCR). Transcript analysis of 11 different $\Delta Os-nadp-me2-3$ mutant lines and the wild type (HY) were performed by RT-PCR (A) and real-time PCR (qPCR) (B). Actin and ubiquitin primers were used as internal controls. $\Delta Os-nadp-me2-3$ (line 3-3) was selected and used for further experimental analysis.



Supplementary Fig. S7. Dead appressorial and hyphal debris were observed on the surface of resistant HY sheath cells after *M. oryzae* inoculation. The remains of oxidized-type dead hyphae and appressorial debris were observed only on the surface of resistant HY sheath cells after inoculation with *M. oryzae* INA168 at 34–48 hpi, whereas successful colonization was observed in susceptible NB and $\Delta Os-nadp-me2-3$. AP, appressorium; IH, invasive hyphae. Scale bars, 10 μ m

TCGAATAAT CAATATCGTA TCCGAGGGGC TCAAGTCTTG TATACTCGAG GCAATGACAT GACCGACCAG CGTTGGAAAC
 TTCAAACATG AACGATGATG ATGACAATGT AAGATCTTCC GAACCAAAAC TCGTCGCATA TTGTTCAGGA AGAGCTGCCC
 GGCAAGCCGT AAAGGAATAT TATTGTTTCTG GCTCTAGACT AACGTCAAAG TGTTTACTTC CCAATCTTCA AGAAACCTTA
 TAGGCTCAAA TATCGACACT AACCCAACCT TGATGTACGC AACATCTTCT CGGTCCAGGT CCCGTCCAG AATCAAACAT
 TCAATCCTGA CTTTCATCTC CTCCTGACCT CCTCTACCGT CAATCTGACT CCCTGCCACG TCCCCACCGC TATGCTCCAG
 GAATTC AAGG CCACTA TCCTA CGAGCTCGTC CTCCCCTTCC GTCCAAAAGC CGCCATTTTG CGAGTCAGTA TCTCCGTCTA
 upstream 1346 forward

CCCAACTCTC TGGGCTGGTG GAGTTCGATG TCGGGGAGTT CGGACTGCTG GACAAGTTTT CAGAGGTTGA AACGCGGCGT
 AGCCTCTCAA AATTTCTTTC CGCTGACACT GATGTAAGTG TAGCGGCCTC TCGTGTTC TCGCCCTCT GAGAGGCCG
 ATGTCACCGA CGCGTTGTGG ATCAAACCTT CCGTGTCTGAA TCTTGGGAAG CAACTATGAG ATGCTTCTAC AACTAAGATA
 upstream-2 inner reverse

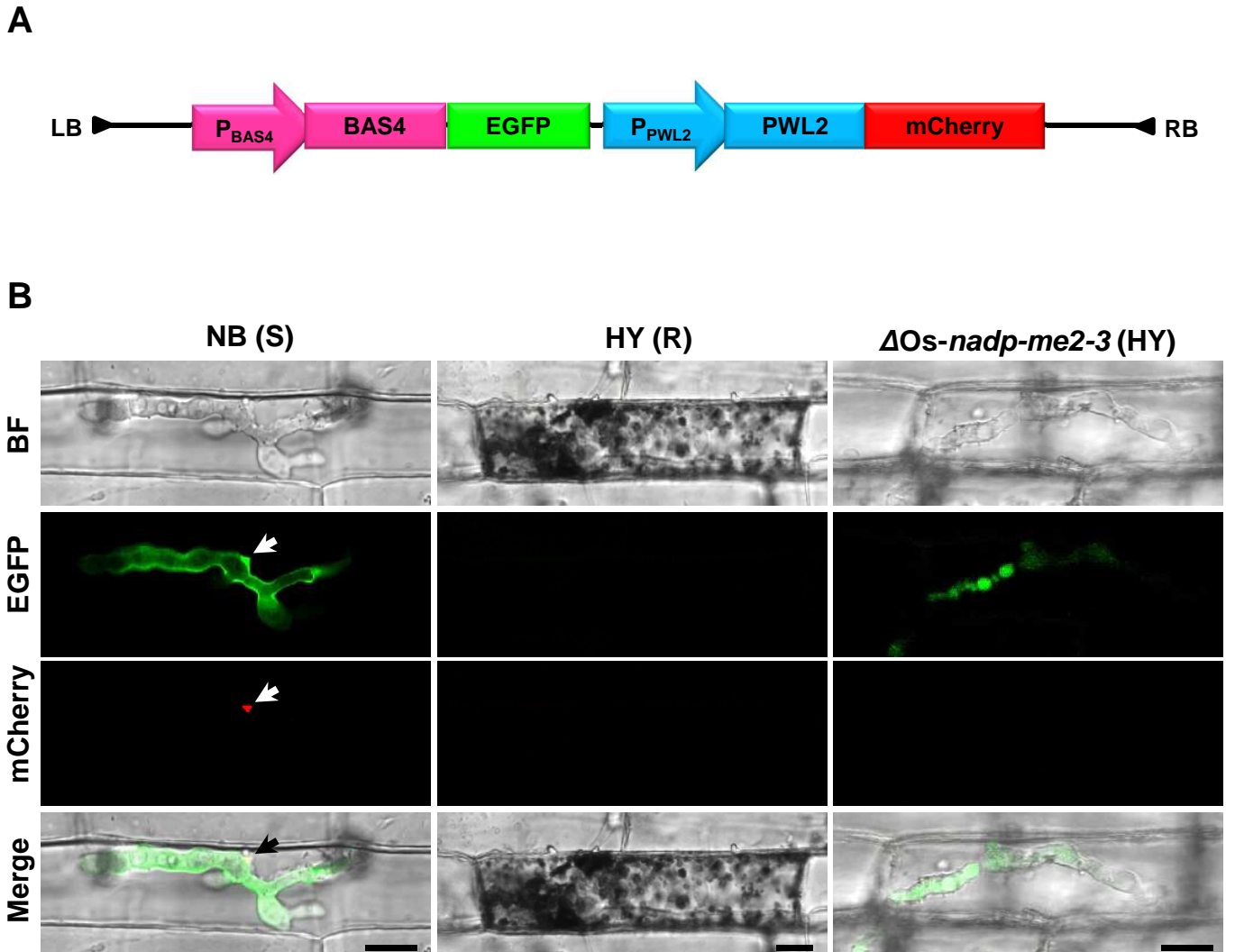
GTAAATTCCT TCTCGGGAAT AGACGGGTAA ACTCTCCAGT CCGATTCTCT AGCTACGGGT TCTTCTGGCA ATGTCCAGAC
 AAGGCATTGC CGCCCTCGA AATCTCCCAT TTGGAATTTT GRTGGCATCA TGTTGTTATC GTCAAACCAG CTCATGACAC
 TGACAGTTTC GGGAGCTTCT TCCTCATCCA TTCGACTATG CGATGGCCGA AAACGACAAA GAATCCGGGT GCGTCCACGA
 upstream-2 outer forward

ACAGACAGAC TCGCGT GCTT TATTGGCCG TATGGATTAC TTTGACTTT TCTTCAATTA TCTTTATTTT AAGTATCGAT
 GTTTTTATA GGTTCGCGT TCCTCTTTT GATTAAATAC TTAAGTATTG TGGTAGATAT CCGCTGACTG GGGGCAACAT
 TGTTGGATT TAAAGTACA TATATAGAAA CGAAAATAAG TGAAAAAGA AGAACAAGAG TAAGGGTTAT TAATTACACG
 ACTAAATGTG GTAATTTAGC TATGTTATAA CCAGGCAAGC ACTACAAATA GCCCAGGGCA ATCAGGAAGA GGCCGATATG
 TTACGATTGA ATAATAAAAT ATTTTATAAA CGTGCATTG GATGTAAATT GTAAATTATG CATTGAGCT CCTCTGCTT
 upstream-1 inner reverse

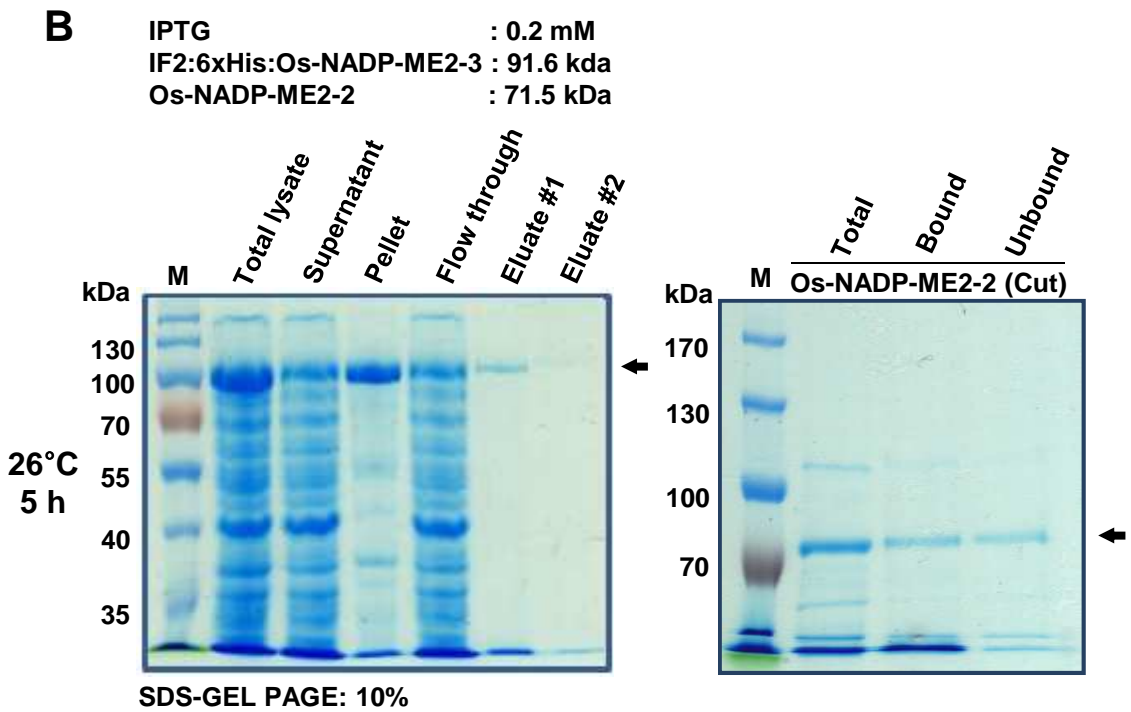
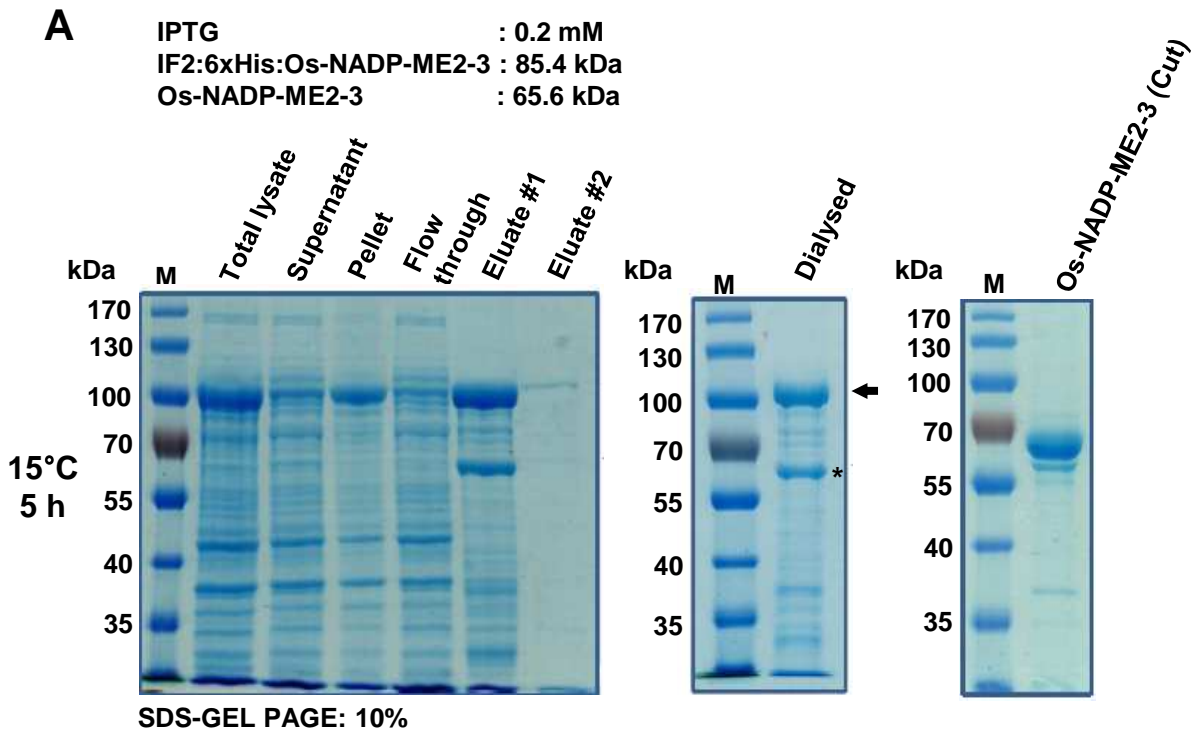
TATTAACAGA AATGTTTTTA AACAGGTAC CTAATGCAA TTCTATATT TTTATGCGGA TTTATGCAGG CCCAAATCCG
 TAGGAAATAC TATTAGTTAT AATAATATAA AAACCTCGGC TTCTGTATA TTAAGTATA ATTCTTTTC TTCCTCTT
 ATATTTTCA TCTTAAAAC AAACATTTAA ATTCTGCTA TTGCAATTATA TGCAATCGGA ATCGCAGCAC TTCCACTCC GGCCAGCCTG
 upstream-1 outer forward

AATGGCAACA CTGAGGTCGC AACCATCTCC GACGTAAAC TTGAGGCCG CAGCGACACC ACTTATCATA AATGCTCAA
 ATGCGTTAT GGCAGCGATG ATTCCGACGC GTATTTAAT CATAAATGCA ACTAA

Supplementary Fig. S8. The genomic structure of the *AVR-Pii* original promoter and coding sequences. The promoter region (1602 bp) was recovered from *M. oryzae* genomic DNA by inverse PCR as described in the Materials and Methods section. Retrotransposon MAGGY (red) is located 1136 bp upstream of the *AVR-Pii* start codon. The coding region of *AVR-Pii* is shown in blue. The primers used for inverse PCR are underlined (purple). The promoter used for *AVR-Pii:mCherry* expression vector construction was 947 bp, as shown in green. The start and stop codons are marked in black squares.



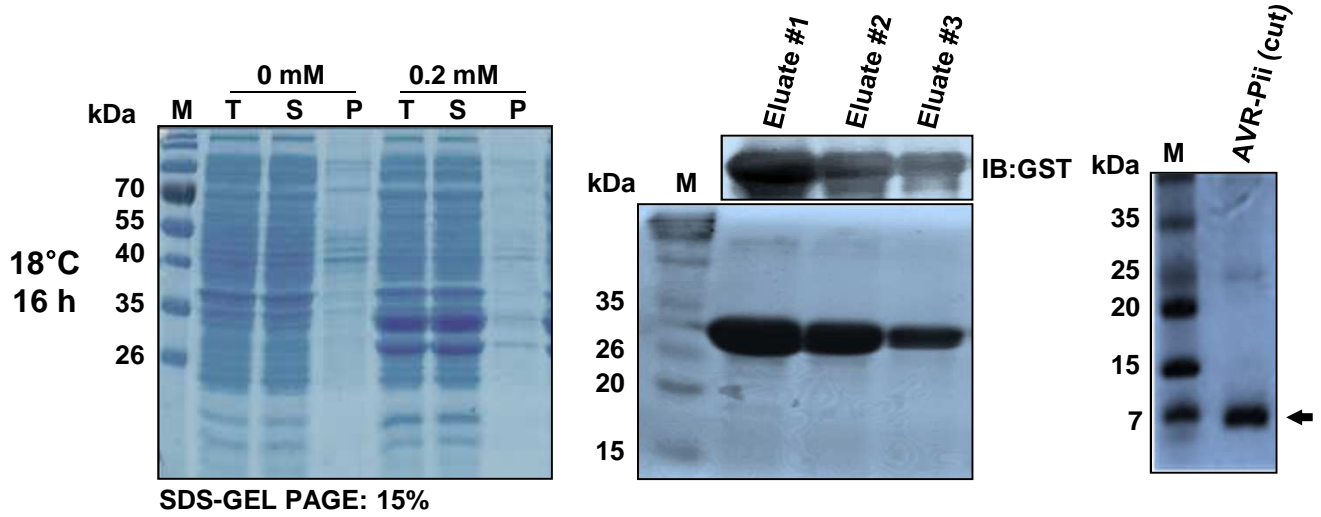
Supplementary Fig. S9. Differential regulation of the effectors was visualized using two BAS4 and PWL2-effector expression cassettes. (A) Schematic representation of plasmid pBV551 containing BAS4:EGFP and PWL2:mCherry as described in the Materials and Methods section. (B) Expression of BAS4 and PWL2 was observed in susceptible NB, where BAS4 appeared uniformly as a bright outline in the invasive hyphae, and PWL2 accumulated locally in the BIC (white arrow) at 34 to 48 hpi. In contrast, expression of BAS4 appeared in invasive hyphae, but PWL2 accumulation was not detected in the $\Delta Os-nadp-me2-3$ mutant. In addition, both BAS4 and PWL2 were not observed in HY, indicating no viable hyphae. BIC, biotrophic interfacial complex; S, susceptible; R, resistant. Scale bars, 10 μ m.



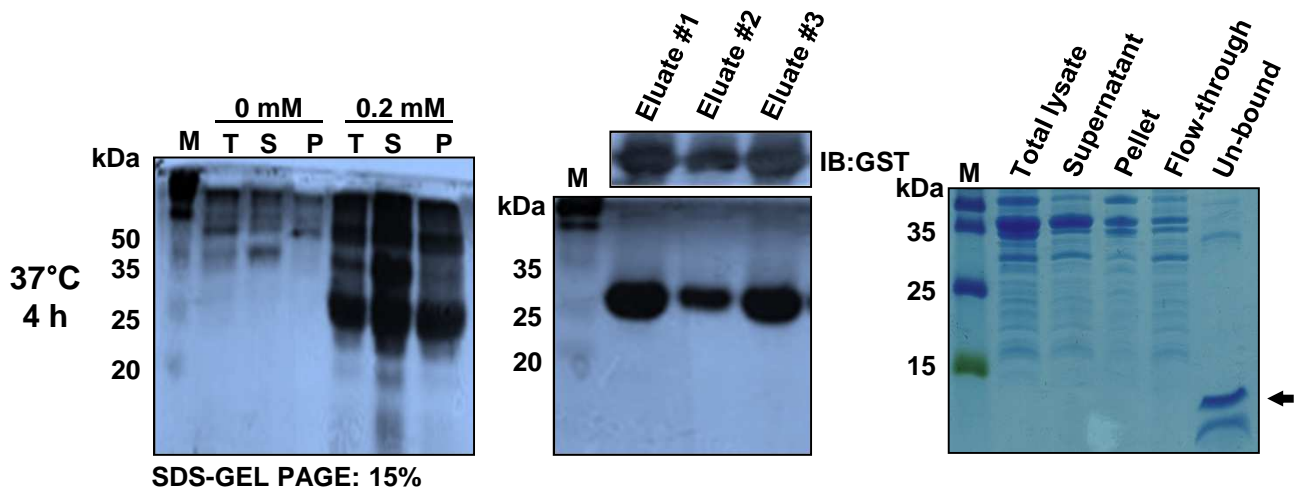
Supplementary Fig. S10. Expression, and purification of N-terminal IF2 and 6×His-tagged OsNADP-ME2-3 and Os-NADP-ME2-2. The pET28a vector was used to express Os-NADP-ME2-3 and Os-NADP-ME2-2 proteins, which provide the N-terminal IF2 and 6×His followed by the thrombin proteolytic site. The total mass of these protein constructs (including the fusion tag) was predicted to be 85.4 kDa for OsNADP-ME2-3 and 91.8 kDa for Os-NADP-ME2-2. (A), (B) Expression and purification of 6xHis:OsNADP-ME2-3 and 6xHis:OsNADP-ME2-2. The protein was induced at 0.2 mM IPTG at 15°C for 5 h and 26°C for 5 h, followed by purification from soluble lysate via nickel affinity chromatography and thrombin digestion. The arrow indicates the full-length protein, whereas the asterisk (*) represents the truncated protein. The protein was run on 10% SDS-PAGE followed by CBB staining. M, protein size marker; P, pellet; S, supernatant; T, total protein.

A

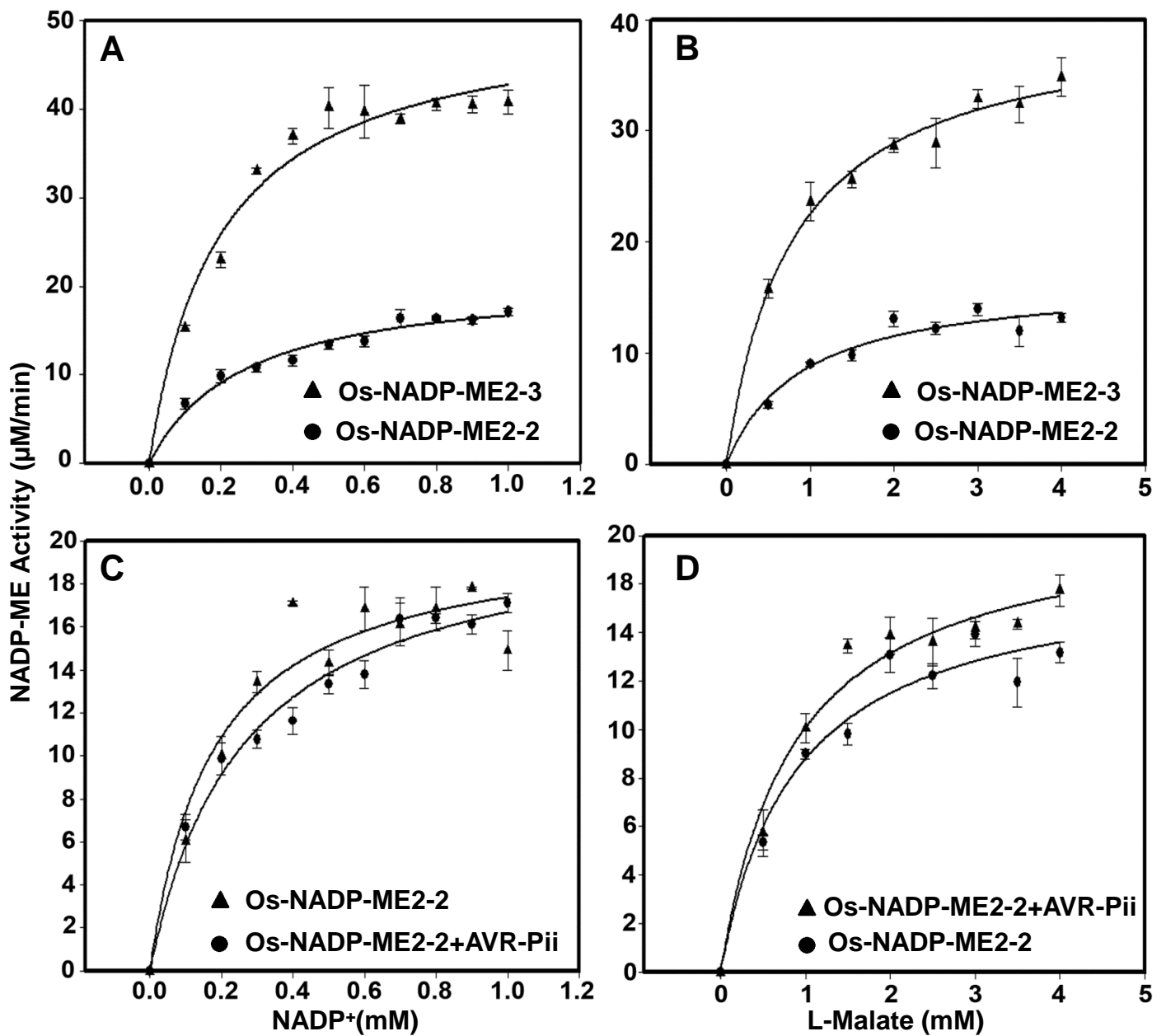
IPTG : 0.2 mM
GST:AVR-Pii : 32.56 kDa
AVR-Pii : 5.66 kDa

**B**

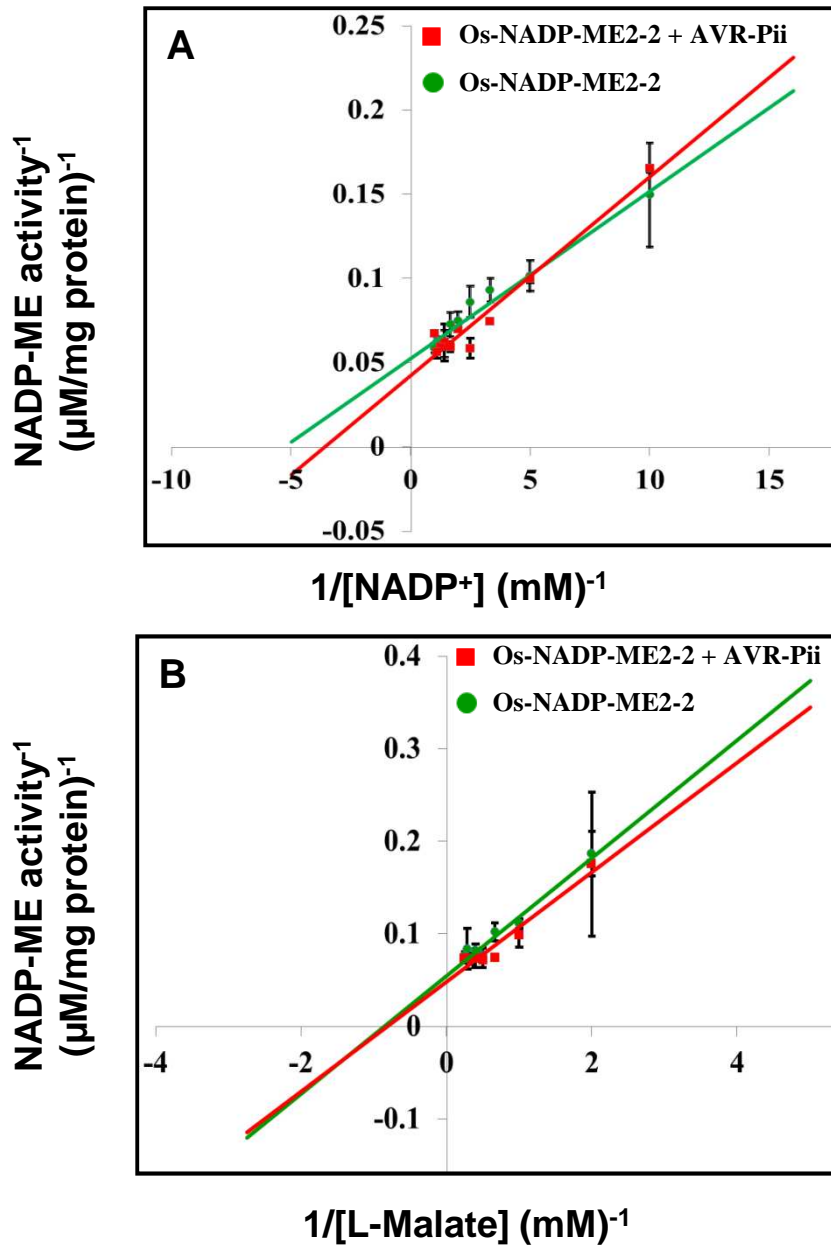
IPTG : 0.2 mM
GST:AVR-Pii-MT : 32.32 kDa
AVR-Pii-MT : 5.42 kDa



Supplemental Figure S11. Expression and purification of N-terminal GST fusion of AVR-Pii and AVR-Pii-MT. pGEX4T-1 was used to express AVR-Pii and AVR-Pii-MT proteins, which provides N-terminal GST followed by the thrombin proteolytic site. The total mass of these protein constructs (including the fusion tag) was predicted to be 32.56 kDa for AVR-Pii and 32.32 kDa for AVR-Pii-MT. (A), (B) Expression and purification of GST:AVR-Pii and GST:AVR-Pii-MT. The protein was induced at 0.2 mM IPTG at 18°C for 16 h and 37°C for 4 h, followed by purification using GST column chromatography from the supernatant and thrombin treatments. The protein was run on 15% SDS-PAGE followed by CBB staining and further confirmed by immunoblotting using anti-GST antibody (1:1000; Santa Cruz Biotechnology, Inc. B-14:sc-138). The purified AVR-Pii and AVR-Pii-MT, after thrombin treatment, were indicated by arrows. M, protein size marker; P, pellet; S, supernatant; T, total protein



Supplemental Figure S12. Os-NADP-ME2-2 show extremely low enzyme activity compared with Os-NADP-ME2-3. (A), (B) The enzyme activity was determined at varying concentrations of NADP^+ at 3.5 mM L-Malate or varying concentrations of L-Malate at 0.3 mM NADP^+ . (C), (D) The activity of Os-NADP-ME2-2 in the presence of 10 nM AVR-Pii at varying concentrations of NADP^+ and L-Malate with fixed levels of the other substrates. The results are presented as the means of triplicate determinants.



Supplemental Figure S13. Double reciprocal plot for inhibition of Os-NADP-ME2-2 activity by AVR-Pii. The activity of Os-NADP-ME2-2 was determined at different concentrations of NADP⁺ (A) and L-malate (B) using the saturation levels of the other substrates. The results show that AVR-Pii does not affect the activity of Os-NADP-ME2-2, suggesting that AVR-Pii has no interaction with the Os-NADP-ME2-2 isoform. The results represent three independent determinants.

Supplemental Table S1. List of AVR-Pii interactors based on Y2H screening using rice cDNA library as prey.

Bait	Prey				
	MSU locus	Given name	Frequency	AA size	Protein localization
AVR-Pii	Os01g52500	Os-NADP-ME	22	496	Cytoplasm
	Os02g30230	Os-Exo70F2	6	689	Cytoplasm
	Os04g31330	Os-Exo70F3	1	688	Nucleus
	Os08g41820	Os-Exo70F4	2	510	Nucleus

Prey

Definition (KOME)	Definition (Genome annotation project)
Malate oxidoreductase, putative similar to malate oxidoreductase (NADP-dependent malic enzyme) GB:P34105 (<i>Populus balsamifera</i> subsp. <i>trichocarpa</i>)	NADP-dependent malic enzyme, putative, expressed
Exocyst subunit EXO70 family protein contains Pfam domain PF03081: Exo70 exocyst complex subunit;	exo70 exocyst complex subunit domain containing protein, expressed
Exocyst subunit EXO70 family protein contains Pfam domain PF03081: Exo70 exocyst complex subunit;	exo70 exocyst complex subunit domain containing protein, expressed
68418.m06240 exocyst subunit EXO70 family protein contains Pfam domain PF03081: Exo70 exocyst complex subunit;	exo70 exocyst complex subunit domain containing protein, expressed

Supplemental Table S2. Kinetic parameters of recombinant Os-NADP-ME2-3 and its isoform Os-NADP-ME2-2.

OsNADP-ME2-3				
	Vmax ($\mu\text{Mmin}^{-1}\text{mg}^{-1}$)	Km (mM)	Kcat (S^{-1})	Kcat/Km ($\text{mM}^{-1} \text{S}^{-1}$)
L-Malate	39.84	0.76	33.2	43.68
NADP⁺	56.17	0.26	46.81	180.04

OsNADP-ME2-2				
	Vmax ($\mu\text{Mmin}^{-1}\text{mg}^{-1}$)	Km (mM)	Kcat (S^{-1})	Kcat/Km ($\text{mM}^{-1} \text{S}^{-1}$)
L-Malate	18.05	1.15	15.04	13.08
NADP⁺	18.9	0.19	15.75	82.89

The indicate kinetic parameters are the mean of three separate determinants with no more than 10% standard deviation.

Supplemental Table S3. Inhibition pattern of Os-NADP-ME2-3 and Os-NADP-ME2-2.

The values are presented as the mean of triplicate determinations with no more than 10% standard deviation.

	Os-NADP-ME2-3		Os-NADP-ME2-2
Varied Substrate	AVR-Pii	AVR-Pii-MT	AVR-Pii
L-Malate	Competitive	N.I.	N.I.
	Ki = 7.6 nM	N.I.	N.I.
NADP ⁺	Competitive	N.I.	N.I.
	Ki = 9.5 nM	N.I.	N.I.

N.I. = No inhibition

Supplemental Table 4. Primers used in this study.

Primer Names		Sequence	Description	
(Os-NADP-ME2-1) Os01g52500.1	Forward	AA AAA GCA GGC TGG TGG AGA GCA	Y2H Screening	
	Reverse	AGA AAG CTG GGT TTA CAA TAC AGG		
(Os-NADP-ME2-2) Os01g52500.2	Forward	AA AAA GCA GGC TGG ATG CGC GCC		
	Reverse	AGA AAG CTG GGT TCA CCG GTA GTT		
(Os-NADP-ME2-3) Os01g52500.3	Forward	AA AAA GCA GGC TGG ATG GAG AGC		
	Reverse	AGA AAG CTG GGT TCA CCG GTA GTT		
(Os-NADP-ME2-4) Os01g52500.4	Forward	AA AAA GCA GGC TGG ATG CAT AAC		
	Reverse	AGA AAG CTG GGT TCA CCG GTA GTT		
AVR-Pii w/o SP	Forward	AA AAA GCA GGC TGG CTT CCC ACT CCG		
	Reverse	AGA AAG CTG GGT TTA GTT GCA TTT		
pDONR	attB1	GGG GAC AAG TTT GTA CAA AAA AGC AGG CT		BiFC cloning
	attB2	GGG ACC ACT TTG TAC AAG AAA GCT GGG T		
AVR-Pii w SP (pEX33)	Forward	<u>TCTAGA</u> ATG CAA CTT TCC AAA ATT	AVR-Pii cloning	
	Reverse	<u>TCTAGA</u> GTT GCA TTT ATG ATT AAA		
AVR-Pii Promoter	Forward-1	<u>GGTACC</u> TTC GCT CTT TTG ATT AAA TAC		
	Forward-2	<u>GTC GAC</u> TGT GGA TCA AAA CTT CCG TGT		
AVR-Pii Promoter Upstream	1-inner-Forward	ACT GAG GTC GCA ACC ATC TC	Inverse PCR for AVR-Pii native promoter cloning	
	1-outer-Forward	CCA AAA TGC AAC TTT CCA AAA		
	1-inner-Reverse	AAG CAG AGG AGC TCA AAT GCA		
	1-outer-Reverse	TAT TTC CTA CGG ATT TGG GC		
	2-inner-Forward	GCT TTA TTT GGC CGT ATG GA		
	2-outer-Forward	TGA CAG TTT CGG GAG CTT C		
	2-inner-Reverse	CCA AGA TTC GAC ACG GAA GT		
	2-outer-Reverse	TGA GGA ATC CGA CTG GAG AG		
	1346-Forward	CCA GGA ATT CAA GGC CAC TA		
BAS4-EGFP	Forward	<u>GTC GAC</u> TCG AGT TCG CTC GGG GGC TGG	BAS4-EGFP construction	
	Reverse	<u>GTC GAC</u> TCT AGT GAT TCT CTA GAT CAT		
AVR-Pii-MT1	Forward	C AGC gct gct TTC gcc GCG TAT TTT AAT CAT AAA TGC	AVR-Pii site-directed mutagenesis	
	Reverse	CGC gcc GGA agc agc GCT GCC ATA ACC GCA TTT GGA G		
AVR-Pii-MT2	Forward	CTT ggc GCC CGC AGC gcc ACC ACT TAT CAT AAA TGC		
	Reverse	GT ggc GCT GCG GGC cgc AAG TTT AAC GTC GGA GAT GGT		
pGEX4T-1	pGEX3	CCG GGA GCT GCA TGT GTC AGA GG		
	pGEX5	GGG CTG GCA AGC CAC GTT TGG TG		
AVR-Pii w/o SP	Forward	GGT TCC GCG T <u>GGATCC</u> CTT CCC ACT CCG GCC AGC	GST pull-down	
	Reverse	AGT CAC GAT <u>GCG GCC GC</u> T TAG TTG CAT TTA TGA TTA		

(Os-NADP-ME2-3) Os01g52500.3	Forward	CGC GCG GCA GCC <u>ATA TG</u> G AGA GCA CCA TGA AG	Os-NADP-ME2-3 protein expression and sequence confirmation
	Reverse	GGT GGT GGT <u>GCT CGA G</u> TC ACC GGT AGT TGC GGT A	
	IntP	GGGCTTGAGATCTTGCC	
(Os-NADP-ME2-2) Os01g52500.2	Forward	CGC GCG GCA GCC <u>ATA TG</u> CGC GCC CTT CGC TCC	Os-NADP-ME2-2 protein expression and sequence confirmation
	Reverse	GGT GGT GGT <u>GCT CGA</u> GTC ACC GGT AGT TGC GGT A	
	IntP	ATATTTAGCCGTCCTCAG	
(Os-NADP-ME2-3) Os01g52500.3	Forward	TAC AGC CCA CTT TAC CGC A ACT	RT-PCR
	Reverse	CGA ACA TAG AAA CAG TAC CGA GAA	
Actin gene	Forward	TCC ATC TTG GCA TCT CTC AG	
	Reverse	GTA CCC GCA TCA GCC ATC TG	
Ubiquitin gene	Forward	GTG GTG GCC AGT AAG TCC TC	
	Reverse	GGA CAC AAT GAT TAG GGA TCA	
(Os-NADP-ME2-3) Os01g52500.3	S4	GTA AGT TGG CAA TGC CAA ATT TTG G	Rice NADP-ME2 deletion mutant genotyping
	RP	GGC AAG CCC CTT GTT GTA GCG	
	RB	TTG GGG TTT CTA CAG GAC GTA AC	

SP, signal Peptide; w/o, without; w, with

